Materials Research Proceedings **26** (2023) 635-640 https://doi.org/10.21741/9781644902431-102

A simple tool to forecast the natural frequencies of thin-walled cylinders

Marco Cammalleri[1,a *], Antonella Castellano[1,b] and Marco Abella[1,c]

[1]Department of Engineering, University of Palermo, Palermo, Italy

[a]marco.cammalleri@unipa.it, [b]antonella.castellano@unipa.it, [c]marco.abella@you.unipa.it

Keywords: Circular Cylindrical Shell, Natural Frequencies, Eigenvalue Problem

Abstract. This paper presents an approximate method to predict the natural frequencies of thin-walled cylinders. By taking inspiration from a previous work of one of the authors, the starting point of the proposed approach is a proper construction of reasonable eigenfunctions. However, a new simple tool based on the principle of virtual work has been developed to estimate the natural frequencies and the amplitude of vibration without complex numerical resolution. Moreover, the applicability of the model is extended to all the most common constraint conditions. The identification of the natural frequencies of a continuous cylinder is reduced to an eigenvalue problem based on a matrix whose elements depend only on the geometric characteristics of the cylinder, the mechanical properties of the material and known numerical parameters. The latter are precalculated for given boundary conditions, covering clamped or pinned end constraints. Although the proposed formulation can address any constraints combination, only a pinned-pinned cylinder is analyzed here for brevity. The reliability of the model was tested against FEM analysis results. These comparisons showed that the maximum error versus the exact solutions for the lowest natural frequency is around 2% for all the mode shapes of the pinned-pinned case, offering an excellent trade-off between accuracy and ease of use.

Introduction

The characterization of the vibratory behaviour of thin-walled cylinders attracts researchers' interest due to the wide use of shells as structural elements in several engineering fields. In particular, predicting their natural frequency is crucial to prevent severe faults during the manufacturing process and the regular use, when time-varying forces often stress these elements.

Due to the continuous nature of thin-walled cylinders, studying their free vibrations is far more complex than a discrete multi-degree-of-freedom system. The integration of the partial differential equations rarely leads to an exact closed-form solution, which, however, is rather convoluted [1]. More frequently, the resolution is achieved by finite element analysis, numerical approaches [1–7] or simplified analytical models [8–12]. Nonetheless, the finite element method (FEM) may require a convergence analysis and lacks intelligibility. On the other hand, advanced numerical techniques enable the resolution of highly accurate models but might be challenging to program, while the introduction of simplifying assumptions allows an analytical solution to the problem at the expense of accuracy.

In contrast, the novel model presented here combines good accuracy with ease of use. It takes inspiration from [9], which provided the natural frequencies by a simple sequence of explicit algebraic equations without the need for complex or iterative numerical resolution. Starting from Love's theory for thin-walled cylinders modified by Reissner and simplified by Donnell's assumptions, the dynamic equilibrium equations are derived as functions of displacements. Then, Hamilton's principle is applied. The assumption of reasonable eigenfunctions, similarly to Rayleigh's method, enables a fast-solving procedure based on the resolution of a cascade of simple algebraic equations. Nonetheless, this method applies only to clamped-clamped cylinders and involves two different sets of eigenfunctions depending on the mode shape order.

In this paper, a reformulation of [9] is proposed. In particular, the equilibrium, compatibility and constitutive equations are the same. Nevertheless, different eigenfunctions are hypothesized at the beginning and the principle of virtual work is used. Moreover, the cascaded algebraic resolutive approach is converted to an eigenvalue problem. The new procedure leads to a faster resolution that can be easily adapted to any constraint condition, not just the clamped-clamped one. By way of example, this paper present only the results for a pinned-pinned cylinder. The reliability of the proposed method is tested by a comparison against FEM analysis results. A maximum error of 2% has been obtained, proving that the model is effective and efficient.

Method

Given a thin-walled circular cylinder having a finite length *l*, constant thickness *h* and mean radius *a* consisting of a material having a density *ρ*, Young's modulus *E* and Poisson's ratio *ν*, Fig. 1 shows the orthogonal local reference system consisting of longitudinal direction *x*, circumferential direction *s* and radial direction *r*.

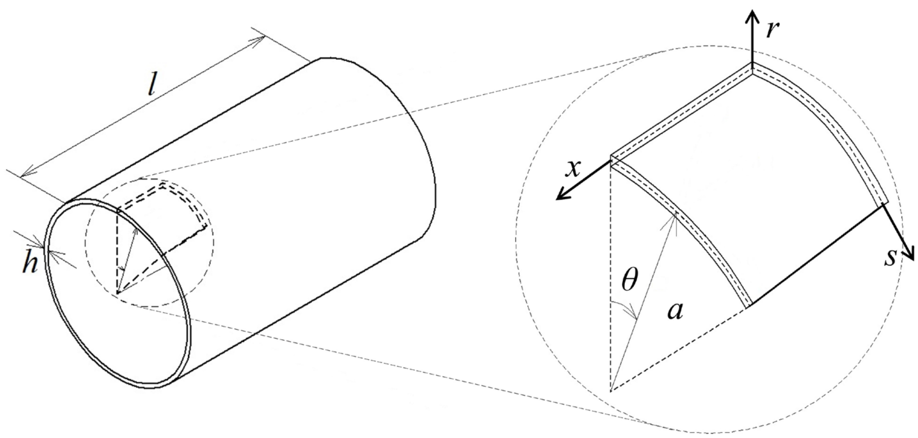

Figure 1. Geometry and local reference system of a thin-walled cylinder.

On the basis of Love's theory [13] modified by Reissner [14] and Donnell's assumptions [15], the dynamic equilibrium equations and the compatibility equations are derived. Then, the constitutive equations are used to express the internal forces and moments as functions of the deformations. After substituting the compatibility equations into these latter equations, forces and moments are obtained as functions of displacements. Then, these forces and moments are introduced into the dynamic equilibrium, and the following equations of motion are obtained:

$$\begin{cases} K\left(\frac{\partial^2 u_x}{\partial x^2} + \frac{1-\nu}{2a^2}\frac{\partial^2 u_x}{\partial \theta^2} + \frac{1+\nu}{2a}\frac{\partial^2 u_s}{\partial x \partial \theta} + \frac{\nu}{a}\frac{\partial u_r}{\partial x}\right) = \rho h \frac{d^2 u_x}{dt^2}, \\ K\left(\frac{1}{a^2}\frac{\partial^2 u_s}{\partial \theta^2} + \frac{1-\nu}{2}\frac{\partial^2 u_s}{\partial x^2} + \frac{1+\nu}{2a}\frac{\partial^2 u_x}{\partial x \partial \theta} + \frac{1}{a^2}\frac{\partial u_r}{\partial \theta}\right) = \rho h \frac{d^2 u_s}{dt^2} \\ K\left[-\frac{\nu}{a}\frac{\partial u_x}{\partial x} - \frac{1}{a^2}\frac{\partial u_s}{\partial \theta} - \frac{u_r}{a^2} - \frac{h^2}{12}\left(\frac{\partial^4 u_r}{\partial x^4} + \frac{1}{a^4}\frac{\partial^4 u_r}{\partial \theta^4} + \frac{2}{a^2}\frac{\partial^4 u_r}{\partial x^2 \partial \theta^2}\right)\right] = \rho h \frac{d^2 u_r}{dt^2} \end{cases} \quad (1)$$

where $K = \frac{Eh}{1-\nu^2}$. The mathematical procedure performed to obtain Eq. 1 is omitted for brevity but can be found in [9]. Nevertheless, if in [9] the equations of motion were used to apply Hamilton's principle, here are introduced in the principle of virtual work (Eq. 2), according to which the virtual work δW of all forces applied to the system, including the inertial actions, is zero for any virtual displacements δu_x, δu_s, and δu_r that meet the constraints.

$$\delta W = aK \int_0^{2\pi} \int_0^{l} \Big\{ \left[\frac{\partial^2 u_x}{\partial x^2} + \frac{1-\nu}{2a^2}\frac{\partial^2 u_x}{\partial \theta^2} + \frac{1+\nu}{2a}\frac{\partial^2 u_s}{\partial x \partial \theta} + \frac{\nu}{a}\frac{\partial u_r}{\partial x} - \frac{1-\nu^2}{E}\rho\frac{d^2 u_x}{dt^2}\right] \delta u_x +$$

$$+\left[\frac{1}{a^2}\frac{\partial^2 u_s}{\partial \theta^2}+\frac{1-\nu}{2}\frac{\partial^2 u_s}{\partial x^2}+\frac{1+\nu}{2a}\frac{\partial^2 u_x}{\partial x \partial \theta}+\frac{1}{a^2}\frac{\partial u_r}{\partial \theta}-\frac{1-\nu^2}{E}\rho\frac{d^2 u_s}{dt^2}\right]\delta u_s + \\ -\left[\frac{\nu}{a}\frac{\partial u_x}{\partial x}+\frac{1}{a^2}\frac{\partial u_s}{\partial \theta}+\frac{u_r}{a^2}+\frac{h^2}{12}\left(\frac{\partial^4 u_r}{\partial x^4}+\frac{1}{a^4}\frac{\partial^4 u_r}{\partial \theta^4}+\frac{2}{a^2}\frac{\partial^4 u_r}{\partial x^2 \partial \theta^2}\right)+\frac{1-\nu^2}{E}\rho\frac{d^2 u_r}{dt^2}\right]\delta u_r\}dxd\theta = 0 \tag{2}$$

Given the arbitrariness of the virtual displacements δu_x, δu_s and δu_r Eq. 2 can be respected only if each of the three addends is null.

Similarly to [9], the assumption of reasonable displacements u_x, u_s and u_r as eigenfunctions of the problem of free vibrations of cylindrical shells enables a simpler approximated mathematical treatment. Free vibrations of a thin-walled circular cylinder consists of *n* circumferential waves and *m* longitudinal half-waves. Therefore, each mode shape is characterized by a pair of values of *n* and *m*. Circumferential waves are independent from the boundary conditions, unlike longitudinal half-waves which, instead, depend on them, similarly to the transverse vibrations of beams subjected to the same constraints. Thus, the same solutions hypothesized in [9], properly chosen to respect orthogonality, are also considered here:

$$\begin{cases} u_x = A_x \frac{d}{dx} f_r(x) cos(n\theta) cos\omega t \\ u_s = A_s f_r(x)\, sin(n\theta)\, cos\omega t \\ u_r = A_r f_r(x) cos(n\theta) cos\omega t \end{cases} \tag{3}$$

where $f_r(x)$ is the eigenfunction of the beam subjected to the same constraints of the cylinder under analysis. For example, for a pinned-pinned beam, $f_r(x) = \sin\beta_i l \frac{x}{l}$, where $\beta_i l$ are the roots of the related frequency equation $\sin\beta_i l = 0$. However, the formulation proposed in the following is highly general and thus can be extended to any boundary conditions.

By normalizing Eq. 2 by the cylinder length *l* and considering Eq. 3, a three-equation system is obtained:

$$\begin{cases} \int_0^1 \left[\left(\frac{\partial^2 u_x}{\partial X^2}+\frac{1-\nu}{2\alpha^2}\frac{\partial^2 u_x}{\partial \theta^2}+\frac{1+\nu}{2\alpha}\frac{\partial^2 u_s}{\partial X \partial \theta}+\frac{\nu}{\alpha}\frac{\partial u_r}{\partial X}+\Delta\, u_x\right)\delta u_x\right]dX = 0 \\ \int_0^1 \left[\left(\frac{1}{\alpha^2}\frac{\partial^2 u_s}{\partial \theta^2}+\frac{1-\nu}{2}\frac{\partial^2 u_s}{\partial X^2}+\frac{1+\nu}{2\alpha}\frac{\partial^2 u_x}{\partial X \partial \theta}+\frac{1}{\alpha^2}\frac{\partial u_r}{\partial \theta}+\Delta\, u_s\right)\delta u_s\right]dX = 0 \\ \int_0^1 \left\{\left[\frac{\nu}{\alpha}\frac{\partial u_x}{\partial X}+\frac{1}{\alpha^2}\frac{\partial u_s}{\partial \theta}+\frac{u_r}{\alpha^2}+\frac{\eta^2}{12}\left(\frac{\partial^4 u_r}{\partial X^4}+\frac{1}{\alpha^4}\frac{\partial^4 u_r}{\partial \theta^4}+\frac{2}{\alpha^2}\frac{\partial^4 u_r}{\partial X^2 \partial \theta^2}\right)-\Delta\, u_r\right]\delta u_r\right\}dX = 0 \end{cases} \tag{4}$$

where $X = \frac{x}{l}$, $\Delta = \frac{1-\nu^2}{E}\rho l^2 \omega^2$, $\alpha = \frac{a}{l}$ and $\eta = \frac{h}{l}$. By substituting Eq. 3 in Eq. 4, the following matrix formulation is derived:

$$\left(\bar{\bar{D}} - \Delta\, \bar{\bar{I}}\right)\{A\} = \{0\} \tag{5}$$

where $\{A\} = \{A_x; A_s; A_r\}$ is the unknown vector containing the displacements amplitudes in the three directions, $\bar{\bar{I}}$ is the identity matrix and $\bar{\bar{D}}$ is the following matrix:

$$\bar{\bar{D}} = \begin{bmatrix} -\frac{I_{13}}{I_{11}}+\frac{1-\nu}{2\alpha^2}n^2 & -n\frac{1+\nu}{2\alpha} & -\frac{\nu}{\alpha} \\ \frac{1+\nu}{2}\frac{n}{\alpha}\frac{I_{02}}{I_{00}} & -\frac{1-\nu}{2}\frac{I_{02}}{I_{00}}+\frac{n^2}{\alpha^2} & \frac{n}{\alpha^2} \\ \frac{\nu}{\alpha}\frac{I_{02}}{I_{00}} & \frac{n}{\alpha^2} & \frac{1}{\alpha^2}+\frac{\eta^2}{12}\left(\frac{I_{04}}{I_{00}}+\frac{n^4}{\alpha^4}-\frac{2}{\alpha^2}n^2\frac{I_{02}}{I_{00}}\right) \end{bmatrix} \tag{6}$$

Materials Research Proceedings **26** (2023) 635-640 https://doi.org/10.21741/9781644902431-102

where $I_{13} = \int_0^1 f_r^1(X)\, f_r^3(X)\, dX$, $I_{11} = \int_0^1 f_r^1(X)\, f_r^1(X)\, dX$, $I_{00} = \int_0^1 f_r(X)\, f_r(X) dX$, $I_{02} = \int_0^1 f_r(X) f_r^2(X)\, dX$ and $I_{04} = \int_0^1 f_r(X) f_r^4(X)\, dX$; $f_r^k(X)$ is the *k*-order derivative of $f_r(X)$. Thanks to the normalization by the cylinder length, these integrals may be evaluated a priori without knowing the actual cylinder dimension. Thus, they need to be calculated only once for any constraint condition and then can be exploited for the free vibrations analysis of any cylinder subjected to the same constraints. Lastly, as it is apparent from Eq. 5, the natural frequency of any thin-walled cylinder can be easily calculated by solving the eigenvalue problem of the matrix $\overline{\overline{D}}$. From the three eigenvalues Δ_1, Δ_2 and Δ_3, the natural frequency is obtained as follows:

$$f_i = \frac{1}{2\pi}\sqrt{\frac{E\Delta}{(1-\nu^2)\rho l^2}} \qquad \text{for } i = 1, 2, 3 \tag{7}$$

To sum up, the proposed analysis of free vibrations of cylindrical shells involves the initial identification of the eigenfunction describing the transverse free vibrations of a beam subjected to the same constraints of the cylinder. Then, a pair of values for *m* and *n* is selected, and the matrix $\overline{\overline{D}}$ is populated. The natural frequencies are evaluated from the eigenvalues of the matrix $\overline{\overline{D}}$, while its eigenvectors contain the displacements amplitude ratios of each modal shape.

Results

Table 1 shows the frequency f_1, f_2 and f_3 for a pinned-pinned cylinder characterized by *a* = 76mm, *l* = 305mm, *h* = 0.254 mm, *ρ* = 7833 kg/m^3, *E* = 207 kN/mm^2, *ν* = 0.3. For brevity, only results for *m* ≤ 3 and *n* ≤ 8 are reported. Nonetheless, they are sufficient to notice that f_1 is lower by un order of magnitude than f_2 and f_3; thus, it is the frequency related to the highest risk of the arising of redundancy condition. Moreover, f_1 shows a minimum for fixed *m*, which occurs for a higher value of *n* if *m* increases, while f_2 and f_3 are monotonically increasing by both *n* and *m*.

Table 1. Natural frequencies for m ≤ 3 and n ≤ 8.

	m = 1			m = 2			m = 3		
n	f_1 [Hz]	f_2 [Hz]	f_3 [Hz]	f_1 [Hz]	f_2 [Hz]	f_3 [Hz]	f_1 [Hz]	f_2 [Hz]	f_3 [Hz]
1	2,886	10,009	17,209	6,445	14,059	21,944	8,556	17,890	29,228
2	1,265	14,889	26,403	3,677	18,061	29,947	5,821	21,647	35,508
3	656	20,923	36,632	2,178	23,194	39,414	3,896	26,222	43,820
4	423	27,319	47,298	1,396	29,012	49,558	2,681	31,491	53,176
5	372	33,847	58,183	985	35,177	60,072	1,931	37,225	63,123
6	431	40,433	69,190	792	41,523	70,807	1,477	43,249	73,434
7	551	47,048	80,272	751	47,971	81,681	1,227	49,455	83,983
8	705	53,681	91,403	819	54,481	92,649	1,132	55,780	94,694

Table 2 shows the amplitude ratios only for *m* ≤ 3 and *n* = 4, but similar trends are obtained for other combinations of *m* and *n*. The predominant amplitude at the lowest natural frequency f_1 is A_r, so the associated motion is mostly radial (transverse mode of vibration). Conversely, at frequencies f_2 and f_3, A_x and A_s prevail, respectively; thus, the associated modes are called longitudinal and circumferential.

Table 2. Amplitude ratios for m ≤ 3 and n = 4.

	$m = 1$		$m = 2$		$m = 3$	
	A_x/A_r	A_s/A_r	A_x/A_r	A_s/A_r	A_x/A_r	A_s/A_r
f_1	0.014	0.252	0.011	0.255	0.008	0.249
f_2	3.697	1.897	1.020	2.155	0.521	2.561
f_3	0.240	4.097	0.259	4.380	0.288	4.822

The accuracy of the results was tested by comparing them against those derived from a FEM analysis carried out in Ansys 2022, where a thin-walled circular cylinder was analyzed using 36,433 SHELL181 linear elements. Fig. 3 and Table 3 reveal a high correspondence between the FEM results and those provided by the proposed model, with a maximum error of 2.07% for m = 1 and n = 6. The comparison considers only the frequency f1 for brevity since it is the lowest.

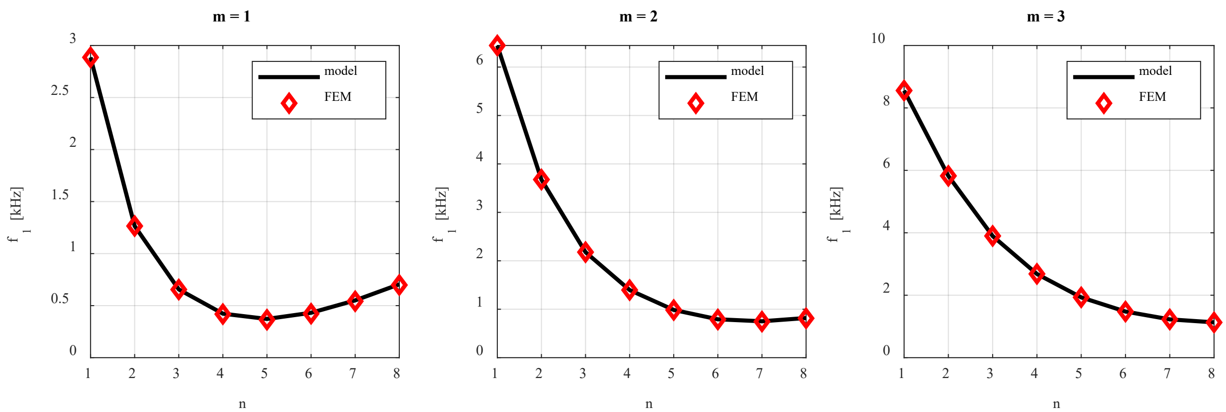

Figure 2. Comparison between the natural frequency f_1 obtained by the model and FEM analysis (m ≤ 3 and n ≤ 8).

Table 3. Percentage error on the f_1 frequency for m ≤ 8 and n ≤ 8.

	$m = 1$	$m = 2$	$m = 3$	$m = 4$	$m = 5$	$m = 6$	$m = 7$	$m = 8$
$n = 1$	-0.0004	-0.0103	-0.0181	-0.0212	-0.0225	-0.0228	-0.0229	-0.0229
$n = 2$	0.0106	-0.0254	-0.0427	-0.0550	-0.0628	-0.0675	-0.0704	-0.0723
$n = 3$	0.1934	-0.0336	-0.0715	-0.0957	-0.1137	-0.1269	-0.1365	-0.1435
$n = 4$	0.9627	0.0093	-0.0921	-0.1365	-0.1681	-0.1927	-0.2120	-0.2222
$n = 5$	2.0088	0.1821	-0.0822	-0.1683	-0.2199	-0.2591	-0.7405	-0.3167
$n = 6$	2.0702	0.5078	-0.0131	-0.1776	-0.2621	-0.3210	-0.3678	-0.9082
$n = 7$	1.5567	0.7645	0.1176	-0.1527	-0.2864	-0.3729	-0.4387	-0.4930
$n = 8$	1.0193	0.7233	0.2303	-0.1016	-0.2895	-0.4100	-0.4991	-0.5714

Conclusions

Starting from the standard equations for modeling equilibrium, deformations and displacements of thin-walled cylinders, this paper used the principle of virtual work to reduce the calculation of the natural frequencies to an eigenvalue problem, thanks to the simplifying assumption of eigenfunctions deduced from the beam theory. The results for a pinned-pinned cylindrical shell were compared to those obtained by a FEM analysis, reporting a maximum error of 2%. Thus, the novel model combines good accuracy with ease of use, being ideal for preliminary investigation of the resonance condition of shell structures. Moreover, it can be potentially extended to any boundary conditions: clamped, pinned, and free end cylinders can be addressed by a unique formulation. Future works will test the model accuracy with other constraints combinations.

References

[1] Y. Xing, B. Liu, T. Xu, Exact solutions for free vibration of circular cylindrical shells with classical boundary conditions, Int. J. Mech. Sci. 75 (2013) 178–188. https://doi.org/10.1016/j.ijmecsci.2013.06.005

[2] Y. Dubyk, I. Orynyak, O. Ishchenko, An exact series solution for free vibration of cylindrical shell with arbitrary boundary conditions, Sci. J. Ternopil Natl. Tech. Univ. 89 (2018) 79–88. https://doi.org/10.33108/visnyk_tntu2018.01.079

[3] Cammarata, A., Sinatra, R., & Maddio, P. D. (2019, July). An extended Craig-Bampton method for the modal analysis of mechanisms. In IFToMM World Congress on Mechanism and Machine Science (pp. 3329-3338). Springer, Cham. https://doi.org/10.1007/978-3-030-20131-9_329

[4] Cammarata, A., Sinatra, R., & Maddìo, P. D. (2019). Static condensation method for the reduced dynamic modeling of mechanisms and structures. Archive of Applied Mechanics, 89(10), 2033-2051. https://doi.org/10.1007/s00419-019-01560-x

[5] M. Cammalleri, E. Pipitone, S. Beccari, G. Genchi, A Mathematical Model for the Prediction of the Injected Mass Diagram of a S.I. Engine Gas Injector, Journal of Mechanical Science and Technology, Springer vol. 11 (2013) pagg. 3253-3265. https://doi.org/10.1007/s12206-013-0848-6

[6] Cammalleri M., Castellano A., Analysis of hybrid vehicle transmissions with any number of modes and planetary gearing: kinematics, power flows, mechanical power losses. Mechanism and Machine Theory 162 (2021) 104350. https://doi.org/10.1016/j.mechmachtheory.2021.104350

[7] S.M.R. Khalili, A. Davar, K. Malekzadeh Fard, Free vibration analysis of homogeneous isotropic circular cylindrical shells based on a new three-dimensional refined higher-order theory, Int. J. Mech. Sci. 56 (2012) 1–25. https://doi.org/10.1016/j.ijmecsci.2011.11.002

[8] C. Wang, J.C.S. Lai, Prediction of natural frequencies of finite length circular cylindrical shells, Appl. Acoust. 59 (2000) 385–400. https://doi.org/10.1016/S0003-682X(99)00039-0

[9] M. Cammalleri, A. Costanza, A closed-form solution for natural frequencies of thin-walled cylinders with clamped edges, Int. J. Mech. Sci. 110 (2016) 116–126. https://doi.org/10.1016/j.ijmecsci.2016.03.005

[10] F. Sorge, M. Cammalleri, Control of hysteretic instability in rotating machinery by elastic suspension systems subject to dry and viscous friction, J. Sound Vib. 329 (2010) 1686. https://doi.org/10.1016/j.jsv.2009.12.007

[11] F. Sorge, M. Cammalleri, On the beneficial effect of rotor suspension anisotropy on viscous-dry hysteretic instability, Meccanica. 47 (2012) 1705–1722. https://doi.org/10.1007/s11012-012-9549-y

[12] A. Kumar, S.L. Das, P. Wahi, Effect of radial loads on the natural frequencies of thin-walled circular cylindrical shells, Int. J. Mech. Sci. 122 (2017) 37–52. https://doi.org/10.1016/j.ijmecsci.2016.12.024

[9] A.E.H. Love, XVI. The small free vibrations and deformation of a thin elastic shell, Philos. Trans. R. Soc. London. 179 (1888) 491–546. https://doi.org/10.1098/rsta.1888.0016

[10] E. Reissner, A New Derivation of the Equations for the Deformation of Elastic Shells, Am. J. Math. 63 (1941) 177. https://doi.org/10.2307/2371288

[11] L.H. Donnell, Beams, plates and shells, McGraw-Hill, New York, 1976.